

## Coordination Chemistry

## Synthesis and Coordination Ability of a Donor-Stabilised Bis-Phosphinidene

Terrance J. Hadlington,<sup>\*,[a, b]</sup> Arseni Kostenko,<sup>[a]</sup> and Matthias Driess<sup>\*,[a]</sup>

**Abstract:** Chelating phosphines have long been a mainstay as efficient directing ligands in transition-metal catalysis. Low-valent derivatives, namely chelating phosphinidenes, are to date unknown, and could lead to chelating complexes containing more than one metal centre due to the intrinsic capacity of phosphinidenes to bind two metal fragments at one P-centre. Here we describe the synthesis of the first such chelating bis-phosphinidene ligand, XantP<sub>2</sub> (**2**), generated by the reduction of a diphosphino xanthene derivative, Xant(PH<sub>2</sub>)<sub>2</sub> (**1**) with <sup>iPr</sup>NHC (<sup>iPr</sup>NHC = [C(N(iPr)C(H))<sub>2</sub>]). Initial studies have shown that this novel chelating ligand can act

as a bidentate ligand towards element dihalides (i.e. FeCl<sub>2</sub>, ZnI<sub>2</sub>, GeCl<sub>2</sub>, SnBr<sub>2</sub>), forming cationic complexes with the tetryl elements. In contrast, XantP<sub>2</sub> demonstrates an ability to bind multiple metal centres in the reaction with CuCl, leading to a cationic Cu<sub>3</sub>P<sub>3</sub> ring complex, with Cu centres bridged by phosphinidene arms. Density Functional Theory calculations show that **2** indeed holds 4 lone pairs of electrons, shedding further light on the coordination capacity for this novel ligand class through observation of directionality and hybridisation of these electron pairs.

## Introduction

The chelate effect describes the binding of a multi-dentate ligand to a metal centre through more than one ligand 'arm'.<sup>[1]</sup> On entropic grounds, this leads to highly stabilised metal complexes, a key factor in generating effective and long-lived catalytically active complexes. Classic examples of neutral chelating ligands are the diphosphino-ethane derivatives,<sup>[2]</sup> with which over 7000 structurally authenticated transition-metal (TM)-complexes have been reported.<sup>[3]</sup> Indeed, these ligands are still broadly employed in catalysis today, as well as in the stabilisation of highly reactive TM fragments.<sup>[2b,4]</sup> Nowadays, a huge number of neutral chelating ligands are known utilizing a number of different donor atoms. In our group, we have focused on the synthesis and employment of chelating bis-silylene ligands, which have proved to be powerful assets in TM

catalysed processes,<sup>[5]</sup> as well as in the stabilisation of reactive complexes of B,<sup>[6]</sup> Ge<sup>0</sup>,<sup>[7]</sup> and Si<sup>0</sup>.<sup>[8]</sup> However, moving beyond the classical chelating ligand structure, we wished to design a system which may accommodate multiple metal centres. In this regard, few examples are known; recent work from Lu et al. has employed tripodal phosphine-functionalised tris-amido ligands, allowing for the systematic design of heterobimetallic complexes.<sup>[9]</sup> Conversely, we chose to explore a chelating ligand where the binding centres have more than one binding site, that is, more than one free pair of electrons. A key class of readily accessible compounds satisfying this characteristic are the NHC-stabilised phosphinidenes,<sup>[10]</sup> which can be seen as inversely polarized phosphalkenes,<sup>[11]</sup> and formally hold two lone pairs of electrons at P.<sup>[12]</sup> Indeed, such species have shown the ability to bind two metals at one P-centre (Figure 1).<sup>[13]</sup> A wide range of carbene-stabilised aryl-phosphinidenes are now known, which are accessed in good yields from

[a] Dr. T. J. Hadlington, Dr. A. Kostenko, Prof. Dr. M. Driess  
Department of Chemistry, Metalorganics and Inorganic Materials  
Technische Universität Berlin  
Strasse des 17. Juni 135, Sekr. C2, 10623 Berlin (Germany)  
E-mail: terrance.hadlington@tum.de  
matthias.driess@tu-berlin.de

[b] Dr. T. J. Hadlington  
Department of Chemistry  
Technische Universität München  
Lichtenbergstraße 4, 85748 Garching (Germany)

Supporting information and the ORCID identification number(s) for the author(s) of this article can be found under:  
<https://doi.org/10.1002/chem.202004300>.

© 2020 The Authors. Chemistry - A European Journal published by Wiley-VCH GmbH. This is an open access article under the terms of the Creative Commons Attribution Non-Commercial License, which permits use, distribution and reproduction in any medium, provided the original work is properly cited and is not used for commercial purposes.

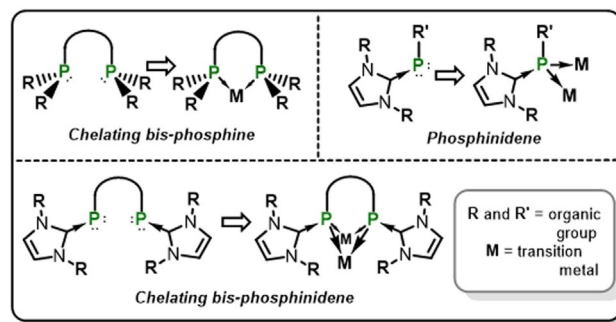


**Figure 1.** Combining the concepts of chelating bis-phosphines and phosphinidenes, coming to the chelating bis-phosphinidenes.

ArPH<sub>2</sub> or ArPCl<sub>2</sub> precursors utilizing NHCs or *s*-block metal reductants, respectively.<sup>[14]</sup> More recently, a number of P<sup>I</sup> compounds have been synthesised through the CO-liberation reaction of the phosphoethynolate ([PCO]) fragment,<sup>[15]</sup> a notable example being the recent isolation of a phosphino-phosphinidene with a monocoordinated terminal P-atom.<sup>[16]</sup> Combining the concepts of classical chelating phosphines with multidentate phosphinidenes, we envisaged that employing two phosphinidene centres in close proximity may allow for the bidentate chelation of two metal centres by a single ligand. We thus targeted the synthesis of a bis-phosphinidene via reduction of a bis-phosphine precursor, and investigations regarding the coordination behaviour of this novel ligand scaffold. Herein we discuss the synthesis of the first isolable example of a chelating bis-phosphinidene ligand, whereby each phosphinidene centre formally holds two lone pairs of electrons. The utilisation of this ligand in the formation of mono-metallic and multi-metallic coordination systems has also been explored, and is discussed.

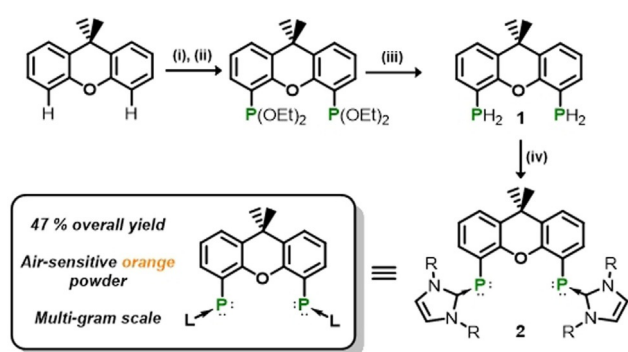
## Results and Discussion

Numerous chelating phosphine systems have been reported in the literature, which typically utilise a readily available scaffold upon which to build the chelating ligand, such as xanthene, ferrocene, and naphthalene.<sup>[17]</sup> Low-cost and easily accessible ligands are desirable, giving the potential for broader usage of these systems in industry and academia. These two key points guided our initial design of a bis-phosphinidene ligand.

As the backbone scaffold for our ligand we chose to develop a xanthene-derived system, given the prominence of ‘Xant-Phos’ in chemical catalysis.<sup>[18]</sup> We also envisaged that the resulting P...P distance would be great enough to disfavour attractive interactions between the P<sup>I</sup> centres. Our synthetic route to the xanthene-derived chelating bis-phosphinidene ligand, **2** (Scheme 1), involved the formal reduction of Xant-(PH<sub>2</sub>)<sub>2</sub> (**1**) with <sup>i</sup>PrNHC (<sup>i</sup>PrNHC = [C{N(*i*Pr)C(H)}<sub>2</sub>]) in the formation of <sup>i</sup>PrNHC-H<sub>2</sub>, which is in close relation to the reduction of PhPH<sub>2</sub> by the same *N*-heterocyclic carbene (NHC), yielding <sup>i</sup>PrNHC→PPh, reported by Radius et al.<sup>[14]</sup> The initial synthesis of **1** is relatively straight forward, following modifications to the proce-

dures reported by Osborn et al. some years ago,<sup>[19]</sup> following double-deprotonation of 9,9-dimethylxanthene with two molar equivs. *n*BuLi in a hexane:diethyl ether mixture.<sup>[20]</sup> In our hands, bis-phosphine derivative **1** could be isolated as a colourless oil through extraction of the crude reaction mixture with Et<sub>2</sub>O following aqueous work up, in 78% yields, and was of adequate purity for subsequent chemistry. Spectroscopic data is lacking in the original publication of this compound, and so is briefly discussed here. The -PH<sub>2</sub> fragments of this species are clearly visible in its <sup>1</sup>H NMR spectrum, presenting as a doublet of multiplets ( $\delta = 4.04$  ppm, <sup>1</sup>J<sub>PH</sub> = 202 Hz; Figure S2 in the Supporting Information), through coupling to P as well as xanthene-Ar protons. Concordantly, the <sup>31</sup>P NMR spectrum (Figure 3) presents a triplet of multiplets, due to Ar-CH couplings; this signal collapses to a singlet in the <sup>31</sup>P{<sup>1</sup>H} NMR spectrum ( $\delta = -140.6$  ppm; Figure S3 in the Supporting Information).

As mentioned, Radius et al. have reported that the addition of <sup>i</sup>PrNHC to PhPH<sub>2</sub> followed by heating to just below reflux in D<sub>8</sub>-toluene leads to the clean formation of <sup>i</sup>PrNHC→PPh.<sup>[14]</sup> We thus hypothesised that a similar approach may be utilised in generating bis-phosphinidene **2** from **1**. Addition of an excess of <sup>i</sup>PrNHC to an NMR sample of **1** in C<sub>6</sub>D<sub>6</sub> leads initially to the formation of a yellow precipitate, which dissolves upon heating the reaction mixture to 65 °C. Continued heating for 2 days leads to the formation of a bright orange solution containing a single new P-containing species ( $\delta = -77.2$  ppm; Figure S7 in the Supporting Information), shifted up-field relative to that for <sup>i</sup>PrNHC→PPh ( $\delta = -59.9$  ppm), but in keeping with the general resonances expected for carbene-stabilised phosphinidenes.<sup>[10b]</sup> Upon cooling of this sample, bright orange crystals of compound **2** readily formed, X-ray diffraction analysis of which confirmed the connectivity in this species (polymorph **2A**, Figure 2). A preparative-scale reaction for the formation of **2** conducted in toluene at 100 °C gave considerably more expedient access to this compound, with the reaction being complete after 12 h as ascertained through NMR spectroscopic analysis. After completion of the reaction, removing all volatiles from the crude mixture and washing with copious amounts of diethyl ether and hexane yielded essential-



**Scheme 1.** The synthesis of bis-phosphinidene ligand **2**. (i) *n*BuLi, 1.0:2/hexane:Et<sub>2</sub>O, 45 °C; (ii) (EtO)<sub>2</sub>PCl, -78 °C-RT; (iii) LiAlH<sub>4</sub>, Me<sub>3</sub>SiCl, -78 °C-RT; (iv) NHC, toluene, 100 °C.

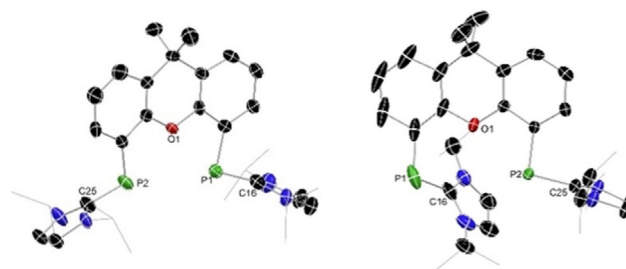


**Figure 2.** Molecular structures of **2A** and **2B**, with probability ellipsoids at 30%, and protons removed for clarity. Selected bond lengths (Å) and angles (°) for **2A**: P1–C16 1.830(5); P2–C25 1.826(6); C16–N1 1.354(7); C16–N2 1.393(7); C25–N3 1.329(8); C25–N4 1.385(8); P1...P2 3.965(2); C2–P1–C16 99.65(3); C12–P2–C25 97.50(2). For **2B**: P1–C16 1.790(5); P2–C25 1.821(3); C16–N1 1.364(5); C16–N2 1.356(5); C25–N3 1.359(4); C25–N4 1.359(4); P1...P2 4.452(1); C16...P2 3.619(4); C2–P1–C16 105.72(2); C12–P2–C25 97.60(1).

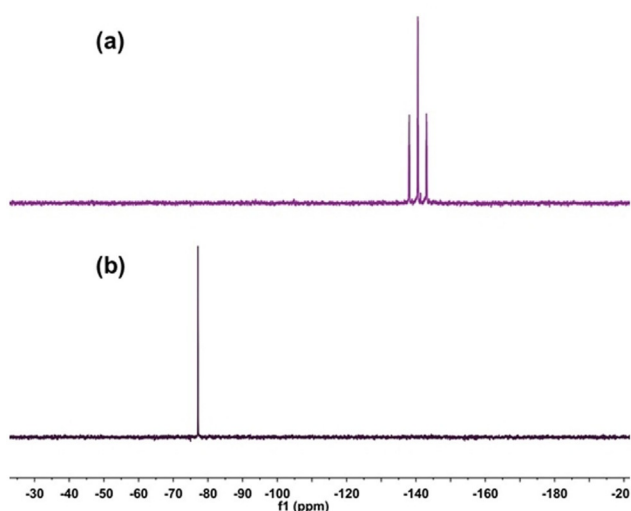


**Figure 3.** (a)  $^{31}\text{P}$  NMR spectrum of bis-phosphine **1**, and (b) bis-phosphinidene **2** in  $\text{D}_6\text{-THF}$ .

ly pure **2** in moderate yields. Figure 3b shows the  $^{31}\text{P}$  NMR spectrum of compound **3**.

Compound **2** is insoluble in hexane, only sparingly soluble in diethyl ether, and rapidly reacts with  $\text{CDCl}_3$ . Upon heating **2** becomes quite soluble in THF, and is readily soluble in acetonitrile at ambient temperatures. Typically, in any solvent, **2** crystallises/precipitates upon modest cooling. We tentatively assign this characteristic to the lattice structure of polymorph **2A** (Figure 2, *left*), where compound **2** appears to form 1D H-bonded chains through the interaction of the NHC backbone-CH moieties of one molecule of **2** with the phosphinidene centres of another. As is perhaps expected, due to the high electron density at the two P centres and their two-coordinate nature, no P...P interaction is apparent in **2A** ( $d(\text{P}\cdots\text{P}) = 3.965(2) \text{ \AA}$ ), with both [CPC] arms sitting essentially coplanar with the xanthene backbone. Notably, recrystallising **2** from dilute THF solutions leads to a second polymorph, **2B** (Figure 2, *right*), in which no strong intermolecular interactions are observed, leading to a monomeric structure. Here the P...P distance is slightly larger than that in **2A** ( $d(\text{P}\cdots\text{P}) = 4.452(1) \text{ \AA}$ ), and one interactions between one P-centre and the NHC C-centre of the  $[\text{C}^{\text{NHC}}\text{-P-C}^{\text{Xant}}$ ] arm is rotated by  $136^\circ$  relative to those in **2A**. It is likely that this conformer is favoured due to intramolecular second  $[\text{C}^{\text{NHC}}\text{-P-C}^{\text{Xant}}$ ] arm, given the inversed polarization of such  $\text{NHC}\rightarrow\text{P}$  moieties leading a positively polarized carbon atom.<sup>[11]</sup> Although the  $\text{P}\cdots\text{C}^{\text{NHC}}$  distance here ( $d(\text{P}\cdots\text{C}^{\text{NHC}}) = 3.619(4) \text{ \AA}$ ) is slightly larger than the sum of the van der Waals radii for these two elements ( $3.5 \text{ \AA}$ ), the overall geometrical parameters perhaps hint towards such an electrostatic interaction.

To gain insight into the above phenomena, the molecular structure of **2** was optimised using Density Functional Theory (DFT), at the B3PW91 level of theory (details in the the Supporting Information). The optimised structure of one molecule of **2** converges to the isolated polymorph **2B**. Furthermore, we were able to identify two additional isomers of **2**, having the  $\text{C}_3$  and  $\text{C}_2$  symmetries. However, both  $\text{C}_3$  and  $\text{C}_2$  isomers are

higher in energy than **2B**, both in gas phase and in solution, by between  $3.7$  and  $4.9 \text{ kcal mol}^{-1}$  (Figure 4). Selected orbitals of **2B** are presented in Figure 4, representing the lone electron pairs available for binding in **2**. The HOMO and HOMO-1 correspond to  $\pi$ -type lone pairs at the phosphorous centres, whilst the HOMO-3 and HOMO-4 correspond to  $\sigma$ -type lone pairs (Figure 5). The corresponding NBOs are presented in Figure S25 (see the the Supporting Information).

With bis-phosphinidene **2** in hand, we wished to explore its use as a ligand towards TM fragments, and further towards to the formation of multi-metallic systems. The addition of a THF suspension of  $\text{ZnI}_2$  to a suspension of **2** in THF rapidly led to complete loss of the bright orange colour of **2**, and the formation of a slightly pale-yellow solution (Scheme 2). A  $^1\text{H}$  NMR spectral analysis of the crude reaction mixture indicated the formation of a single new product. Crystals isolated from a concentrated THF extract of the reaction mixture were confirmed to be the 1:1 coordination product, **3**, through an X-ray diffraction analysis (Figure 6). Compound **3** contains a tetrahe-

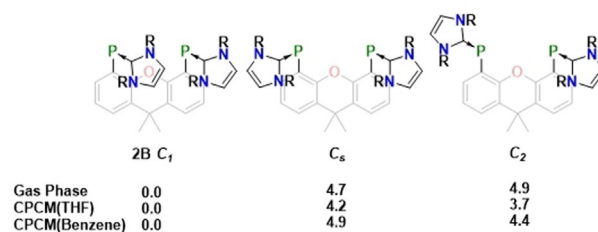


**Figure 4.** Calculated relative energies for isomers of **2**.

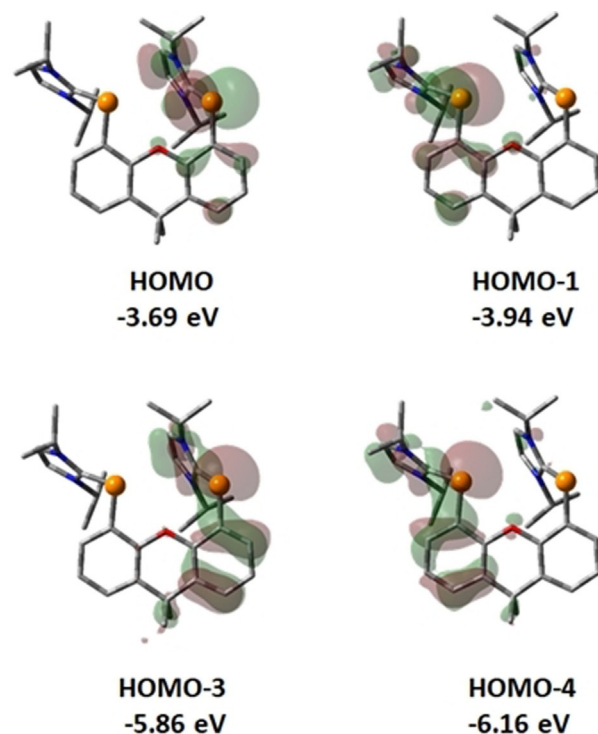
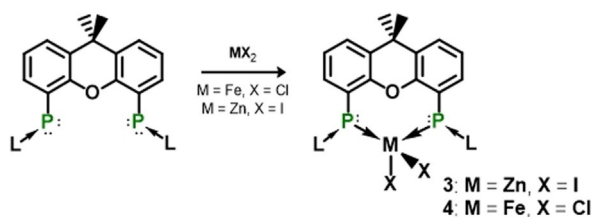


**Figure 5.** Selected orbitals of **2B**.



**Scheme 2.** Synthesis of 1:1 TM complexes, **3** and **4**, utilising bis-phosphinidene **2**.

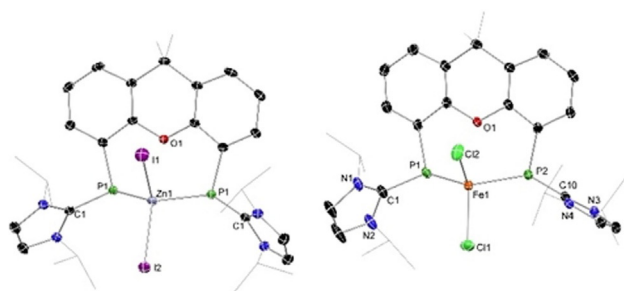


**Figure 6.** Molecular structures of **3** (left) and **4** (right) with 30% probability ellipsoids, and H atoms removed for clarity. Selected bond lengths (Å) and angles ( $^{\circ}$ ) for **3**: P1–Zn1 2.433(4); P1–C1 1.827(4); C1–N1 1.362(5); C1–N2 1.366(6); P1–Zn1–P1' 101.23(1); C1–P1–Zn1 111.19(5); Zn1–P1–C10 103.76(4). For **4**: P1–Fe1 2.471(2); P2–Fe1 2.490(1); P1–C1 1.828(5); P2–C10 1.832(5); P1–Fe1–P2 103.10(5); C1–P1–Fe1 109.87(2); C10–P2–Fe1 114.32(2); Fe1–P1–C20 105.46(2); Fe1–P2–C30 103.11(2).

dral coordinated  $\text{Zn}^{\text{II}}$  centre, bound by two iodide ligands, and the two P centres of the bis-phosphinidene ligand. The xanthen backbone in **3** is planar, however, both P centres hold a trigonal-pyramidal geometry indicative of stereoactive lone pairs of electrons. Both Zn–P–C<sup>Xant</sup> angles are equal due to a symmetry plane through the centre of its molecular structure ( $103.76(4)^{\circ}$ ), and are surprisingly acute, with both carbene donors sitting out-of-plane relative to the xanthen backbone. This is further borne out by the C<sup>Xant</sup>–P...P–C<sup>NHC</sup> torsion angles, which deviate considerably from linearity ( $44.13(8)^{\circ}$ ). This effectively forms an open binding pocket on the open face of the bis-phosphinidene ligand. Despite this apparent ‘open pocket’, addition of a further equivalent of  $\text{ZnI}_2$  to **3** does not lead to formation of the desired bis-adduct. In fact, addition of a second metal dihalide, namely  $\text{FeCl}_2$ , to THF solutions of **3** does not lead to a heterobimetallic complex, but rather to  $\text{ZnI}_2$  displacement, and formation of yellow solutions of XantPP– $\text{FeCl}_2$  (**4**, Scheme 2). This species is also quantitatively formed upon addition of  $\text{FeCl}_2$ , as a suspension in THF, to bis-phosphinidene **2**. The  $^1\text{H}$  NMR spectrum of **4** dissolved in  $\text{D}_8$ -THF is extremely broadened due to paramagnetism, whilst the  $^{31}\text{P}$  NMR spectrum is silent. Compound **4** crystallises from concentrated THF or acetonitrile solutions as yellow crystals, with a molecular structure similar to that for **3** (Figure 6). That is, C<sup>Xant</sup>–P–Fe angles are near-right-angles ( $105.46(2)$  and  $103.11(2)$ ), and considerable torsion of the NHC units away from the xanthen plane can be observed ( $39.1(4)^{\circ}$  and  $54.6(4)^{\circ}$ ). Addition of further  $\text{FeCl}_2$  does not lead to the complexation of a second equivalent of this metal halide.

A DFT analysis of **3** hints as to why the desired bis-metallated species are geometrically inaccessible, with selected orbitals depicted in Figure 7. The HOMO and the HOMO-1 correspond to the dative interactions between the two phosphorus centres and Zn, with the HOMO-10 and HOMO-11 corresponding to the remaining pairs of electrons at the two phosphorous centres, presenting as  $\sigma$ -type lone pairs. The NBO diagram of the participating orbitals is presented in Figure S26 in the Supporting Information). These latter  $\sigma$ -type lone pairs lie perpendicular to the xanthen plane, and thus parallel to each other, therefore not allowing for the chelation of a second metal. It is likely, however, that either utilising a more flexible backbone, or a backbone leading to reduced P...P distance, could circumvent this situation.

Similar to the  $\text{ZnI}_2$  displacement observed upon addition of  $\text{FeCl}_2$  to **3**, we also observed that the addition of  $\text{CuCl}$  to either **3** or **4** in acetonitrile leads to Zn/Fe displacement, respectively, and formation of the cluster  $[(\text{XantP}_2)\text{Cu}_3\text{Cl}_2]^+\text{Cl}^-$  (**5**). Interestingly, we found that the 1:1 addition of  $\text{CuCl}$  to XantP<sub>2</sub> led to the same cluster complex, as did the 2:1 addition, indicating a considerable relative stability of **5** over the 1:1 and 2:1 XantP<sub>2</sub>:CuCl complexes. The  $^1\text{H}$  NMR spectrum of **5** at ambient temperature is highly complex, featuring a number of essentially indistinguishable broad peaks, indicative of the unsymmetrical nature of this species. In keeping with this, the  $^{31}\text{P}$  NMR spectrum of **5** at ambient temperature also shows a number of broad signals. Satisfyingly, however, heating this sample to  $60^{\circ}\text{C}$  shows a clean coalescence of signals in the  $^1\text{H}$  NMR spectrum, leading to assignable signals (Figure S14 in the Supporting Information). Similarly, the  $^{31}\text{P}$  NMR spectrum also coalescence to a single peak at this temperature ( $\delta = -95.5$  ppm; Figure S14 in the Supporting Information), sug-

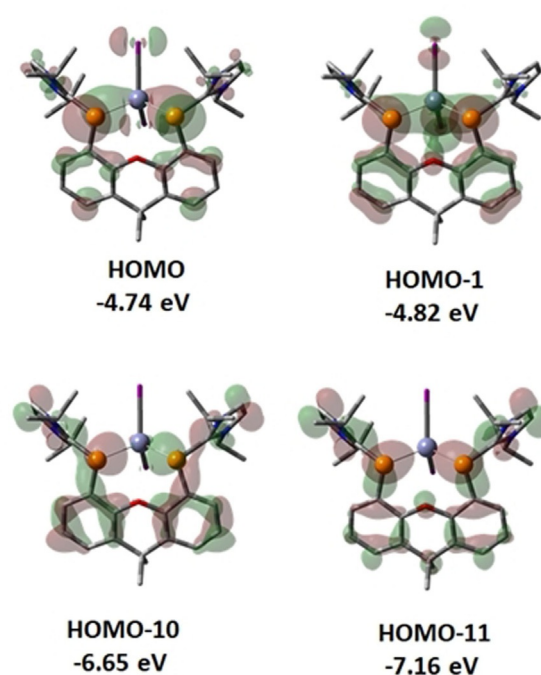


**Figure 7.** Selected orbitals of **3**.



gesting to some degree rapid ligand exchange processes upon heating samples of **5** in solution. Cooling the sample returns the highly complicated spectra observed prior to heating. This  $^{31}\text{P}$  NMR signal for **5** is considerably shifted to higher field than previously reported NHC-phosphindene complexes of a  $\text{CuCl}$ ,<sup>[13d,21]</sup> perhaps indicating a greater donor strength for the phosphindene centres in **2** relative to previously reported examples. Isolated crystals of compound **5** contained considerable amounts of highly disordered solvent in the crystal lattice, which led to the acquisition of data of below publishable quality. This precludes a discussion of specific structural parameters in the molecular structure of **5**, but does confirm its connectivity (Figure 8).

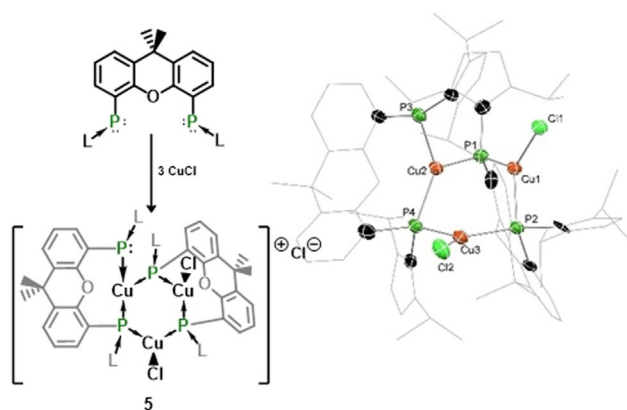


**Figure 8.** Molecular structure of the cationic part of **5** with 30% probability ellipsoids, and H atoms removed for clarity. Metrical parameters are excluded due to low crystal quality.

Unlike compounds **3** and **4**, the molecular structure of compound **5** demonstrates the capacity of the bis-phosphindene ligand **2** to act as a tetra-dentate chelating ligand. Of the four P-centres in **5**, three are found bridging two Cu-centres, forming a six-membered ring structure, which, given the above described NMR spectra, is likely labile. All Cu centres are three-coordinate, two being bound by two P centres and a chloride, and the third by three P centres, resulting in the formation of a cationic Cu centre and a free chloride counter ion. This structural motif is in contrast to previously reported mono or bis- $\text{CuCl}$  adducts of NHC-phosphindenes, which are monomeric, or show bridging  $\text{CuCl}\cdots\text{CuCl}$  interactions, in the solid state.<sup>[21]</sup> However, the molecular structure of **5** is reminiscent of reported trimeric  $\text{Ph}_2\text{PCu}$  complexes, (i.e.  $[\text{L}\rightarrow\text{CuPPH}_2]_3$ ;  $\text{L} = \text{DippNHC}$  or 1,10-phenanthroline;  $^t\text{BuNHC} = [\text{C}(\text{N}(\text{tBu})\text{C}(\text{H})_2)_2]$ ,<sup>[22]</sup> and perhaps even more so to the  $\text{CuCl}$  complex of an inversely polarised phosphalkene reported by Weber et al.,<sup>[23]</sup> all of which hold a six-membered  $\text{Cu}_3\text{P}_3$  core with alternating Cu and P atoms.

Following from the synthesis of TM systems utilising bis-phosphindene **2**, we sought related chemistry involving low-valent group 14 fragments (Figure 9). To this end,  $\text{GeCl}_2$ -dioxane was reacted with **2**. Addition of THF to a rapidly stirred mixture of this dihalide and **2** led initially to dissolution of the solids, followed by precipitation of a pale yellow

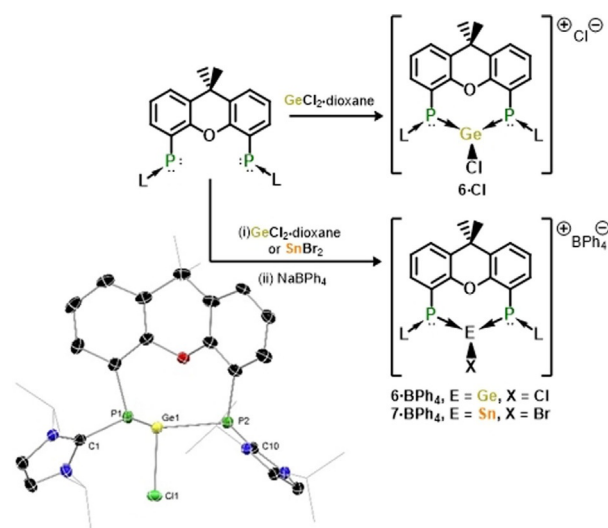


**Figure 9.** Synthesis of cationic adduct complexes **6** and **7**, and the molecular structure of the cationic part of **6-BPh<sub>4</sub>** with 30% probability ellipsoids, and H atoms removed for clarity. Selected bond lengths (Å) and angles (°): P1–Ge1 2.507(3); P2–Ge1 2.488(4); C1–P1 1.842(8); P2–C10 1.831(6); P1–Ge1–P2 94.70(1); C1–P1–Ge1 98.49(2); C10–P2–Ge1 101.06(2); C20–P1–Ge1 101.18(2); C30–P2–Ge1 97.80(2).

powder after a few minutes. This was presumed to be due to the formation of the salt separated ion pair, that is,  $[\text{2-GeCl}]^+ \text{Cl}^-$ , based on similar results reported previously for the combination of strongly donating bidentate ligands with group 14 element dihalides.<sup>[24]</sup> Layering an acetonitrile solution of  $\text{GeCl}_2$ -dioxane with a solution of **2** in the same solvent led to the formation of large crystals after 12 h at ambient temperature. The molecular structure ascertained from these crystals confirmed our hypothesis regarding the formation of separated ion pairs, leading to Ge complex **6-Cl** (Figure 9). This contrasts with reported chelating bis-phosphine complexes of  $\text{GeCl}_2$ , which typically form neutral, four-coordinate species,<sup>[25]</sup> indicating the strong coordination ability of **2**. Notably, the  $\text{Cl}^-$  counterion in **6-Cl** is readily exchanged upon reaction of this complex with  $\text{NaBPh}_4$  in acetonitrile, leading to **6-BPh<sub>4</sub>**. In conjunction with this, the consecutive addition of  $\text{SnBr}_2$  and  $\text{NaBPh}_4$  to a solution of **2** in acetonitrile led to the analogous complex of  $\text{BrSn}^+$ , namely **7-BPh<sub>4</sub>** (Figure 8). To the best of our knowledge, these complexes represent the first examples of phosphindene-coordinated tetrylene species. Both  $\text{BPh}_4$  species could be crystallised from acetonitrile, although due to considerable disorder in the  $\text{BPh}_4$  anion, the crystallographic data for **7-BPh<sub>4</sub>** are insufficient for discussion. Nevertheless, the collected data confirm the connectivity in this species (Figure S1 in the Supporting Information). In the solid state, the cationic part of **6** and **7** are essentially isostructural, and all feature the central E-X fragment disordered over two positions, with this bond sitting parallel above the xanthenene plane, or rotated by  $180^\circ$  in the plane of the xanthenene backbone. This backbone is considerably puckered in all three species when compared with the described TM complexes **3** and **4**, seemingly due to the near-acute P-E-P angles in the tetrylene complexes (**6-Cl**:  $98.13(3)^\circ$ ; **6-BPh<sub>4</sub>**:  $94.72(1)^\circ$ ), compared with the

more open angles in **3** (angle<sub>P1-Zn1-P2</sub> = 101.24(2)°) and **4** (angle<sub>P1-Fe1-P2</sub> = 103.10(5)°). P-E distances are in keeping with known dative P→E single bonds. As with complexes **3** and **4**, addition of further EX<sub>2</sub> species (E = Ge, Sn; X = halide) to **6** or **7** did not lead to complexation, again due to the structure of these complexes 'opening' the binding angle of the opposite face of the phosphinidene ligand to too great a degree. Taken as a whole, however, these initial results are a highly promising starting point to explore the further utility of this novel bis-phosphinidene ligand scaffold.

## Conclusions

In conclusion, we report the initial synthesis of the readily accessible chelating bis-phosphinidene ligand **2**, and have probed its complexation reactivity in conjunction with Cu, Fe, Zn, Ge, and Sn halides. In the former case, the ability for **2** to bind multiple metal centres at each P centre has been demonstrated, whilst complexes with Ge<sup>II</sup> and Sn<sup>II</sup> halides readily form ion separated pairs. We are currently further exploring the unusual coordination chemistry of this ligand class towards further metals, and in the formation of easily accessible hetero-multimetallic systems.

## Experimental Section

Experimental procedures and characterization data for all new compounds, full details of the computational studies, crystal data, and details of data collections and refinements are available in the Supporting Information. General experimental considerations and the synthesis of compound **2** are outlined below.

**General considerations:** All experiments and manipulations were carried out under dry oxygen free dinitrogen using standard Schlenk techniques or in an MBraun inert atmosphere glovebox containing an atmosphere of high purity dinitrogen. Hexane, toluene, diethyl ether, THF, and acetonitrile were dried by standard methods. C<sub>6</sub>D<sub>6</sub>, CD<sub>3</sub>CN, and D<sub>8</sub>-THF were stirred over a sonicated potassium mirror for a period of 48 h and recondensed into a Schlenk tube containing activated 4 Å mol sieves. NMR spectra were recorded on a Bruker AV 200, 400, or 500 Spectrometer. The <sup>1</sup>H and <sup>13</sup>C{<sup>1</sup>H} NMR spectra were referenced to the residual solvent signals as internal standards. <sup>11</sup>B NMR spectra were externally calibrated with BF<sub>3</sub>·OEt<sub>2</sub> (15% in CDCl<sub>3</sub>); <sup>31</sup>P NMR spectra were externally calibrated with H<sub>3</sub>PO<sub>4</sub> (85% in H<sub>2</sub>O). The starting material NHC (NHC = [C(N(*i*Pr)C(H))<sub>2</sub>]) was synthesized according to the known literature procedure.<sup>26</sup> All other reagents were used as received.

**Synthesis of 2:** Compound **1** (2 g, 7.3 mmol) was dissolved in toluene (75 mL), and NHC added (2.2 mL, 14.6 mmol) via syringe. A yellow precipitate immediately formed. The reaction mixture was then heated to 100 °C and kept at this temperature without stirring for 10 h, after which time no solid was present and the solution had become an intense bright orange colour. A <sup>31</sup>P NMR analysis of this solution indicated that all of compound **1** had been consumed. The reaction mixture was cooled to room temperature, and all volatiles removed in vacuo. The oily orange residue was washed multiple times with Et<sub>2</sub>O (4 × 20 mL) and hexane (2 × 20 mL) to remove excess NHC and the by-product, NHC-H<sub>2</sub>, leaving an analytically pure bright orange powder, **2** (2.52 g, 60%). X-ray quality crystals of **2** were obtained by slow-cooling of a hot, satu-

rated solution of **2** in either THF or a benzene/THF mixture, giving two different polymorphs. <sup>1</sup>H NMR (D<sub>8</sub>-THF, 200 MHz, 298 K): δ = 1.24 (d, <sup>3</sup>J<sub>HH</sub> = 6.8 Hz, 24H, NHC-*i*Pr-CH<sub>3</sub>), 1.53 (s, 6H, Xant-(CH<sub>3</sub>)<sub>2</sub>), 4.99 (sept, <sup>3</sup>J<sub>HH</sub> = 6.8 Hz, 4H, NHC-*i*Pr-CH), 6.54 (m, 2H, Xant-Ar-H), 6.84 (m, 4H, Xant-Ar-H), 7.08 (s, 4H, NHC-(*i*Pr)NCH); <sup>13</sup>C{<sup>1</sup>H} NMR (D<sub>8</sub>-THF, 75.5 MHz, 298 K): δ = 22.5 (NHC-*i*Pr-CH<sub>3</sub>), 33.1 (NHC-*i*Pr-CH), 35.1 (Xant-CH<sub>3</sub>), 50.0 and 50.1 (NHC-(*i*Pr)NCH), 116.2, 119.5, 122.0, 128.9, and 130.7 (Xant-Ar-C); <sup>31</sup>P NMR (D<sub>8</sub>-THF, 162 MHz, 298 K): δ = 77.2; HR MS (SI): *m/z* = 575.3064 (calcd for [M+H]<sup>+</sup>: 575.3069).

**Crystallographic data:** Deposition numbers 2022087 (**2A**), 2022088 (**2B**·1 (THF)), 2022089 (**3**·2 (CH<sub>3</sub>CN)), 2022090 (**4**·1 (THF)), 2022091 (**4**·2 (CH<sub>3</sub>CN)), 2022092 (**6**·Cl·1 (CH<sub>3</sub>CN)) and 2022093 (**6**·BPh<sub>4</sub>) contain(s) the supplementary crystallographic data for this paper. These data are provided free of charge by the joint Cambridge Crystallographic Data Centre and Fachinformationszentrum Karlsruhe Access Structures service.

## Acknowledgements

This work was funded by the DFG (German Research Foundation) under Germany's Excellence Strategy—EXC 2008—390540038—UniSysCat and DR-226-17/3. Open access funding enabled and organized by Projekt DEAL.

## Conflict of interest

The authors declare no conflict of interest.

**Keywords:** bimetallic · catalysis · chelating ligands · main group elements · phosphinidene

- [1] a) *The Chelate Effect in Werner Centennial* (Ed.: A. E. Martell), American Chemical Society, New York, **1967**; b) J. J. R. Frausto da Silva, *J. Chem. Educ.* **1983**, *60*, 390–392.
- [2] a) *Phosphines: preparation, reactivity and applications in Organophosphorus Chemistry: Vol. 48* (Eds.: E. I. Musina, A. S. Balueva, A. A. Karasik), Royal Society of Chemistry, London, **2019**; b) *Homogeneous Catalysis with Metal Phosphine Complexes* (Ed.: L. M. Pignolet), Springer, Heidelberg **1983**.
- [3] As ascertained by a survey of the CCDC.
- [4] a) C. A. Laskowski, A. J. M. Miller, G. L. Hillhouse, T. R. Cundari, *J. Am. Chem. Soc.* **2011**, *133*, 771–773; b) S. Imm, S. Bähn, M. Zhang, L. Neubert, H. Neumann, F. Klasovsky, J. Pfeffer, T. Haas, M. Beller, *Angew. Chem. Int. Ed.* **2011**, *50*, 7599–7603; *Angew. Chem.* **2011**, *123*, 7741–7745.
- [5] a) Y.-P. Zhou, M. Driess, *Angew. Chem. Int. Ed.* **2019**, *58*, 3715–3728; *Angew. Chem.* **2019**, *131*, 3753–3766; b) A. Kostenko, M. Driess, *J. Am. Chem. Soc.* **2018**, *140*, 16962–16966; c) Y. Wang, A. Kostenko, S. Yao, M. Driess, *J. Am. Chem. Soc.* **2017**, *139*, 13499–13506; d) Y. Wang, A. Kostenko, T. J. Hadlington, M.-P. Luecke, S. Yao, M. Driess, *J. Am. Chem. Soc.* **2019**, *141*, 626–634.
- [6] H. Wang, L. Wu, Z. Lin, Z. Xie, *J. Am. Chem. Soc.* **2017**, *139*, 13680–13683.
- [7] Y. Wang, M. Karni, S. Yao, Y. Apeloig, M. Driess, *J. Am. Chem. Soc.* **2019**, *141*, 1655–1664.
- [8] Y. Wang, M. Karni, S. Yao, A. Kaushansky, Y. Apeloig, M. Driess, *J. Am. Chem. Soc.* **2019**, *141*, 12916–12927.
- [9] a) P. A. Rudd, S. Liu, N. Planas, E. Bill, L. Gagliardi, C. C. Lu, *Angew. Chem. Int. Ed.* **2013**, *52*, 4449–4452; *Angew. Chem.* **2013**, *125*, 4545–4548; b) R. C. Cammarota, L. J. Clouston, C. C. Lu, *Coord. Chem. Rev.* **2017**, *334*, 100–111.
- [10] a) A. J. Arduengo III, H. V. R. Dias, J. C. Calabrese, *Chem. Lett.* **1997**, *26*, 143–144; b) T. Krachko, J. C. Slootweg, *Eur. J. Inorg. Chem.* **2018**, 2734–

- 2754; O. Back, M. Henry-Ellinger, C. D. Martin, D. Martin, G. Bertrand, *Angew. Chem. Int. Ed.* **2013**, *52*, 2939–2943; *Angew. Chem.* **2013**, *125*, 3011–3015.
- [11] L. Weber, *Eur. J. Inorg. Chem.* **2000**, 2425–2441.
- [12] A. J. Arduengo III, C. J. Carmalt, J. A. C. Clyburne, A. H. Cowley, R. Pyati, *Chem. Commun.* **1997**, 981–982.
- [13] a) A. Doddi, D. Bockfeld, T. Bannenberg, P. G. Jones, M. Tamm, *Angew. Chem. Int. Ed.* **2014**, *53*, 13568–13572; *Angew. Chem.* **2014**, *126*, 13786–13790; b) A. Doddi, D. Bockfeld, A. Nasr, T. Bannenberg, P. G. Jones, M. Tamm, *Chem. Eur. J.* **2015**, *21*, 16178–16189; c) D. Bockfeld, A. Doddi, P. G. Jones, M. Tamm, *Eur. J. Inorg. Chem.* **2016**, 3704–3713; d) C. M. E. Graham, C. R. P. Millet, A. N. Price, J. Valjus, M. J. Cowley, H. M. Tuononen, P. J. Ragogna, *Chem. Eur. J.* **2018**, *24*, 672–680.
- [14] H. Schneider, D. Schmidt, U. Radius, *Chem. Commun.* **2015**, *51*, 10138–10141.
- [15] For a recent review discussing these reactions and broader [PCO] chemistry, see: J. M. Goicoechea, H. Grützmacher, *Angew. Chem. Int. Ed.* **2018**, *57*, 16968–16994; *Angew. Chem.* **2018**, *130*, 17214–17240.
- [16] a) L. Liu, D. A. Ruiz, D. Munz, G. Bertrand, *Chem.* **2016**, *1*, 147–153; b) M. M. Hansmann, R. Jassar, G. Bertrand, *J. Am. Chem. Soc.* **2016**, *138*, 8356–8359.
- [17] a) S. Hillebrand, J. Bruckmann, M. W. Haene, *Tetrahedron Lett.* **1995**, *36*, 75–78; b) J. J. Bishop, A. Davison, M. L. Katcher, D. W. Lichtenberg, R. E. Merrill, J. C. Smart, *J. Organomet. Chem.* **1971**, *27*, 241–249; c) R. D. Jackson, S. James, A. G. Orpen, P. G. Pringle, *J. Organomet. Chem.* **1993**, *458*, C3–C4.
- [18] a) M.-N. Birkholz née Gensow, Z. Freixa, P. W. N. M. van Leeuwen, *Chem. Soc. Rev.* **2009**, *38*, 1099–1118; b) P. W. N. M. van Leeuwen, P. C. J. Kamer, *Catal. Sci. Technol.* **2018**, *8*, 26–113.
- [19] P. Dierkes, S. Ramdeehul, L. Barloy, A. De Cian, J. Fischer, P. C. J. Kamer, P. W. N. M. van Leeuwen, J. A. Osborn, *Angew. Chem. Int. Ed.* **1998**, *37*, 3116–3118; *Angew. Chem.* **1998**, *110*, 3299–3301.
- [20] M. Hirotsu, N. Ohno, T. Nakajima, C. Kushibe, K. Uenob, I. Kinoshita, *Dalton Trans.* **2010**, *39*, 139–148.
- [21] V. A. K. Adiraju, M. Yousufuddin, H. V. R. Dias, *Dalton Trans.* **2015**, *44*, 4449–4454.
- [22] a) C. Meyer, H. Grützmacher, H. Pritzkow, *Angew. Chem. Int. Ed. Engl.* **1997**, *36*, 2471–2473; *Angew. Chem.* **1997**, *109*, 2576–2578; b) J. Yuan, L. Zhu, J. Zhang, J. Li, C. Cui, *Organometallics* **2017**, *36*, 455–459.
- [23] L. Weber, J. Krümborg, H.-G. Stämmler, B. Neumann, *Z. Anorg. Allg. Chem.* **2004**, *630*, 2478–2482.
- [24] a) Y. Xiong, S. Yao, S. Inoue, A. Berkefeld, M. Driess, *Chem. Commun.* **2012**, *48*, 12198–12200; b) Y. Xiong, S. Yao, G. Tan, S. Inoue, M. Driess, *J. Am. Chem. Soc.* **2013**, *135*, 5004–5007; c) C. Gendy, A. Mansikkamäki, J. Valjus, J. Heidebrecht, P. C.-Y. Hui, G. M. Bernard, H. M. Tuononen, R. E. Wasylishen, V. K. Michaelis, R. Roesler, *Angew. Chem. Int. Ed.* **2019**, *58*, 154–158; *Angew. Chem.* **2019**, *131*, 160–164; d) J. Schröder, T. Böttcher, *Eur. J. Inorg. Chem.* **2020**, 342–348.
- [25] F. Cheng, A. L. Hector, W. Levason, G. Reid, M. Webster, W. Zhang, *Inorg. Chem.* **2010**, *49*, 752–760.
- [26] T. Schaub, M. Backes, U. Radius, *Organometallics* **2006**, *25*, 4196–4206.

---

Manuscript received: September 22, 2020

Revised manuscript received: October 23, 2020

Accepted manuscript online: October 26, 2020

Version of record online: December 23, 2020